FEBS Letters 423 (1998) 86–92 FEBS 19838

Four conductance levels of cloned cardiac L-type Ca^{2+} channel α_1 and α_1/β subunits

N. Gondo[a], K. Ono[a,*], K. Mannen[b], A. Yatani[c], S.A. Green[d], M. Arita[a]

[a] *Department of Physiology, Oita Medical University, 1-1 Idaigaoka, Hasama, Oita 8795503, Japan*
[b] *Department of Experimental Animal Facilities, Oita Medical University, Hasama, Oita 8795503, Japan*
[c] *Department of Pharmacology and Cell Biophysics, University of Cincinnati College of Medicine, Cincinnati, OH 451267, USA*
[d] *Department of Medicine, University of Cincinnati College of Medicine, Cincinnati, OH 451267, USA*

Received 2 January 1998

Abstract Formation of single channel subconductance is one of the unique characteristics of the L-type Ca^{2+} channel. Although α_1 subunit exhibits a primary function of the channel, it remains uncertain whether α_1 subunit alone is able to produce subconductance. We tested this by studying single channel currents of cloned cardiac α_1 subunit expressed in Chinese hamster fibroblast cells, with/without coexpression of cardiac β subunit. The α_1 subunit exhibited four distinct levels of conductance (22.7, 14.3, 6.2 and 3.2 pS). Coexpression of β subunit significantly increased the number of openings in all four levels of conductance without changing the conductance values.

Key words: Calcium channel; Subconductance; α Subunit; β Subunit; Chinese hamster fibroblast; Dihydropyridine

1. Introduction

The dihydropyridine (DHP)-sensitive L-type cardiac calcium (Ca^{2+}) channel comprises four subunits: α_1, β and α_2/δ. The pore-forming α_1 subunit involves the most important functional elements of the L-type Ca^{2+} channel including a selectivity filter, voltage sensor, and binding site for DHP [1]. The functional role of the α_2/δ subunit is less clear; some investigators [2,3] reported that it modifies the α_1 subunit function so that activation times of the barium current decreased twofold, while others [4] claimed that the α_2 subunit played a role in Ca^{2+}-dependent inactivation. The rat cardiac type β subunit (β_2), first cloned from rat brain which is ~10 kDa larger than the skeletal muscle counterpart [5], is now recognized to be identical to the rabbit cardiac β subunit (CaB2a) [6]. The cardiac α_1 subunit current, generated by interactions with or without specific β subunits, has been studied with a variety of expression systems. Coexpression of the skeletal β subunit (β_1) with cardiac α_1 subunit (α_{1c}) increased the density of L-type Ca^{2+} current [2,3,7,8], increased the rate of inactivation [2,9,10], and increased the density of maximum DHP binding sites [2,7–11]. Homologous coexpression of the cardiac α_1 subunit (α_{1c}) with the cardiac β subunit (β_{2a}) increased both the amplitude of Ba^{2+} current and the rate of channel activation [6,13]. Moreover, Ca^{2+} currents of the combination of the cardiac $\alpha_1+\alpha_2$ subunits were increased in the presence of the brain/cardiac β subunit (β_3) [13]. This suggests that, although their structures are different, β_1, β_2 and β_3 subunits play similar regulatory roles in the kinetic modulation of channel openings by interacting with α_1.

Subconductance levels when studying Ca^{2+} channels have so far only been clearly seen with L-type Ca^{2+} channels [14]. Although the α_1 subunit exhibits a primary function common to that of the native L-type Ca^{2+} channel, it remains uncertain whether the α_1 subunit alone is able to produce multiple conducting states seen in L-type Ca^{2+} channels. Furthermore, much less is known of the function of the β subunit in forming channel conductance and subconductance. The question is whether the α_1 subunit alone is able to produce multiple conducting states and whether the β subunit coexpressed with α_1 affects the evolution of subconductance levels. We therefore performed experiments using Chinese hamster fibroblast (CHW) cells permanently transfected with cDNA of the cardiac α_1 subunit alone or of the α_1 subunit together with the cardiac β_{2a} subunit. A preliminary report has appeared in abstract form [15].

2. Materials and methods

2.1. Cell transfection and cell culture

Chinese hamster fibroblast (CHW 1102) cells were maintained in Dulbecco's modified Eagle medium (DMEM) supplemented with 10% fetal calf serum (FCS), 100 U/ml penicillin and 100 μg/ml streptomycin, in an atmosphere of 95% O_2 plus 5% CO_2 at 37°C. CHW cells were stably transfected either with class 1C-a (rabbit cardiac) α_1 subunit alone (CHW α_1) or with class 1C-a α_1 subunit and β type 2 (rabbit cardiac β_{2a}) subunit (CHW α_1/β) of the L-type calcium channel. Construction of plasmids carrying the cDNAs encoding the cardiac α_1 and cardiac β subunits have been described previously [16,17]. cDNA encoding of the rabbit cardiac L-type Ca^{2+} channel α_1 subunit [3] inserted into the mammalian expression vector pKNH and rabbit cardiac L-type Ca^{2+} channel β_{2a} subunit cDNA [18] subcloned into p912023(B) were kindly provided by Dr. L. Birnbaumer. CHW cells were cotransfected with 20 μg α_1/pKNH and 20 μg β_{2a}/p912023(B) using the calcium phosphate precipitation method. Transfected cells were selected because of their resistance to DMEM supplemented with 10% dialysed FCS and 300 μg/ml G418 (a neomycin analogue). Expression of detectable mRNA for α_1 and α_1/β subunits was previously confirmed in our stable cell lines (α_1 cell, α_1/β cell) by Northern analysis [17], and lack of any detectable mRNA for these subunits in untransfected CHW cells was also confirmed by Northern analysis [17].

2.2. Electrophysiology

For electrophysiological measurements, cells were seeded onto glass coverslips and incubated for 1–3 days in culture medium with FCS. Patch-clamp current recordings (List EPC-7, Germany) were made in the cell-attached configuration [19]. Patch pipettes with resistances ranging between 0.5 and 1.5 MΩ were used to record currents from patches having 1–3 channels. In step-pulse protocols, patches were depolarized for 195 ms (or 395 ms every 3.33 s) from a holding potential of −80 mV. In a ramp-pulse protocol, patches were promptly depolarized from a holding potential of −80 mV to +40

*Corresponding author. Fax: (81) (975) 49-6046.
E-mail: ono@oita-med.ac.jp

PII S0014-5793(98)00070-2

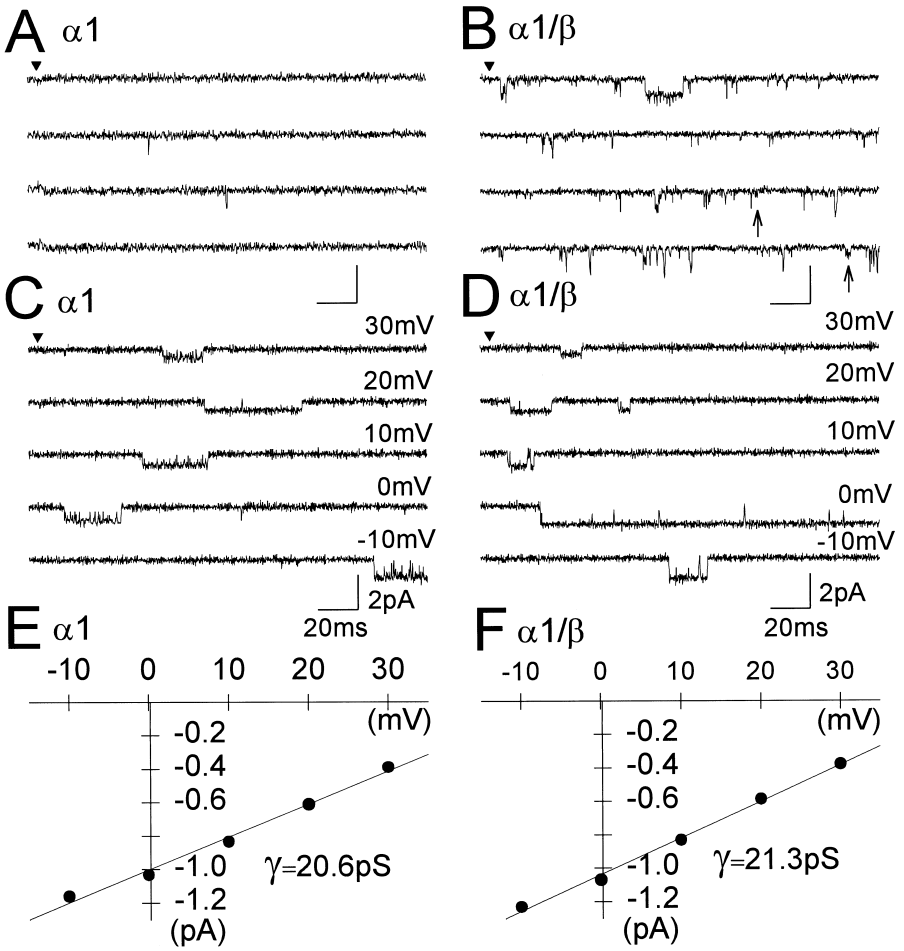

Fig. 1. Single cardiac α_1 and α_1/β Ca^{2+} channel recordings from cell-attached patches expressed in CHW 1102 cells, with 110 mM Ba^{2+} as a charge carrier in the pipettes. A: Four consecutive traces of the α_1 subunit channel obtained in response to 195 ms depolarizing pulses to a 0 mV test potential from a holding potential of −80 mV. Onset of the voltage step is indicated by a solid triangle. B: Four consecutive traces of the α_1/β subunit channel with the same protocol as in A. Arrows indicate typical activities with smaller unitary amplitude (minor openings) than the other openings with full size (major openings). C: Individual traces of the α_1 channel current upon step depolarization from −80 mV to various potentials labeled on the right of each trace. Bay-K 8644 (5 μM) was included in the pipette. D: Individual traces of the α_1/β channel currents, in the presence of Bay-K 8644 (5 μM) with the same voltage clamp protocol as in C. E: Current-voltage (I-V) relationship made from the amplitude histograms of the α_1 channel, collected from the experiments shown in C. A linear regression line of the data indicates a single channel conductance of 20.6 pS in this patch and 22.5 ± 0.2 pS in 12 patches from 12 cells. F: Current-voltage relationship of the α_1/β channel made from the amplitude histograms collected from the experiments shown in D. Single channel conductance was 21.3 pS in this patch, and 22.2 ± 0.2 pS in 25 patches from 25 cells.

mV for 100 ms, and then repolarized slowly to the holding potential at −0.1 V/s. Experimental protocols and data acquisition were performed with a DOS-based 486 microcomputer programmed with ASYST (Asyst, New York). Channel currents were 8-pole Bessel filtered at 2 kHz and digitized at 12 bits at 10 kHz or 20 kHz. Current sweeps were leak- and capacity-compensated using an average of sweeps with no activity (nulls) at each test potential. Transitions between closed and open levels were determined by using a threshold detection algorithm which required that two data points exist above the half mean amplitude of the single-unit opening. Computer-detected openings were confirmed by visual inspection and sweeps having excessive noise were discarded. Amplitude histograms were constructed from corrected traces with a bin width of 48.4 fA, and single channel current was measured as the mean value from a Gaussian function fitted to the amplitude histogram. Voltage (mV)-single channel current (i) relations and individual ramp-sweeps were fitted by linear least-square regression lines, and single channel (sub)conductances were obtained by the slopes of the regression lines. For some ramp-clamp sweeps, a smoothing algorithm was applied to remove noise. This function generated a data sequence that was the arithmetic mean by averaging the series in the window range of 5 (i.e. $n_k = (n_k + n_{k+1} + n_{k+2} + n_{k+3} + n_{k+4})/5$). All experiments were performed at room temperature (20–23°C). Data are expressed as the mean ± standard deviation (n = number of observations) wherever possible.

2.3. Solutions

The bath for the current recording contained 140 mM K-aspartate and 10 mM HEPES (pH adjusted to 7.4 with CsOH). This solution was assumed to collapse the membrane potential so that the applied potential was considered to be the patch membrane potential. The pipette solution contained 110 mM $BaCl_2$, 10 mM tetraethylammonium chloride (TEA-Cl), 10 mM HEPES, 0.3 mM 4,4′-diisothiocyanostilbene-2,2′-disulfonic acid (DIDS) and 0.05 mM tetrodotoxin (TTX) (pH adjusted to 7.4 with TEA-OH). Some experiments (Fig. 4) utilized a pipette solution containing 110 mM NaCl, 10 mM TEA-Cl, 10 mM HEPES, 1 mM EGTA, 0.3 mM DIDS and 0.05 mM TTX (pH adjusted to 9.0 with NaOH). TEA^+, DIDS and TTX were added to block any existing endogenous K^+, Cl^- and Na^+ channels. In some experiments (see Section 3), Bay-K 8644 (5 μM, Calbiochem) was added to the pipette solution (from a 10 mM stock solution of Bay-K 8644 dissolved in 100% ethanol). Freshly prepared BAPTA-AM (1 mM, Calbiochem) was applied from the bath solution in experiments (see Section 3). All other chemicals were purchased from Sigma Chemical Co.

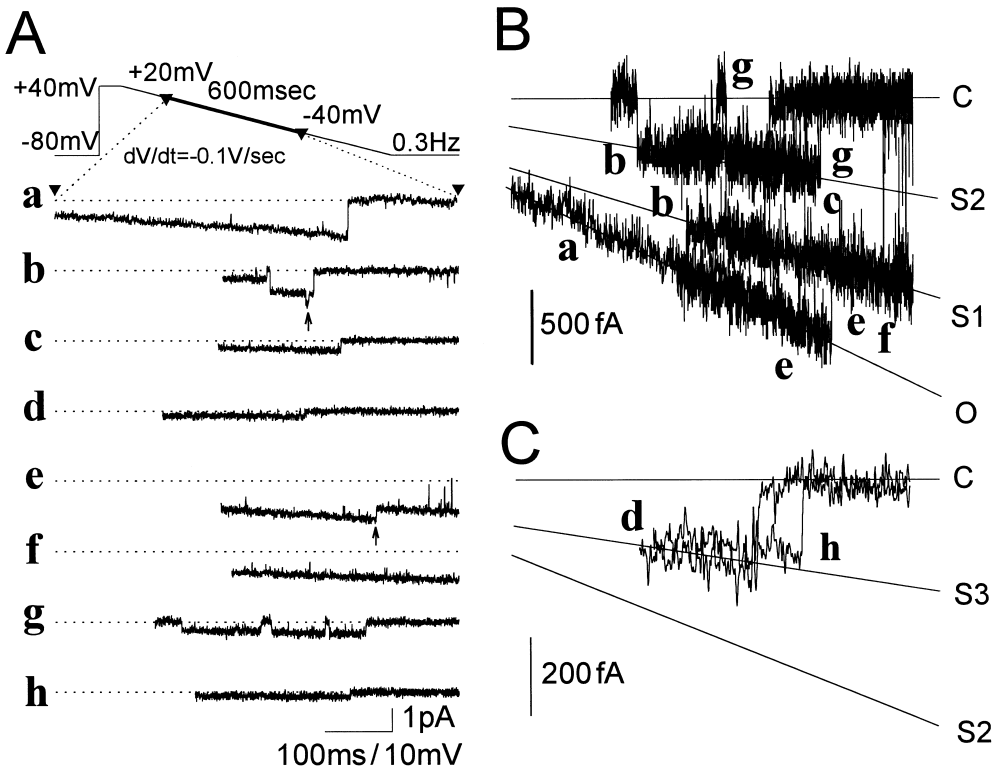

Fig. 2. Illustration of different unitary current amplitudes, recorded during application of a ramp voltage clamp in cell-attached configuration. A: Single channel activity recorded during application of a 600 ms ramp pulse from +20 mV to −40 mV (see upper insert). Traces a–d were obtained from an α_1 channel, while traces e–h were from an α_1/β channel. Dashed lines indicate the closed level. B: Superimposed traces of a–c and e–g in A, made using the same time and voltage scale (cf. bottom calibration in A) and enlarged current scale. Linear regression lines (O, S1, S2) revealed three distinct open states. The closed level (C) is also indicated by a continuous line. C: Superimposed traces of d and h in A, with greatly enlarged vertical scale. For clarity, a digital smoothing algorithm was applied to reduce current noise. Regression of S3 indicates the presence of an additional much smaller open state level. Bay-K 8644 (5 μM) was included in the pipette solution throughout the experiments.

3. Results

Transfection of CHW 1102 cells with cDNA encoding either the α_1 or α_1 plus β subunits of the cardiac Ca^{2+} channel have led to the stable expression of functional L-type Ca^{2+} channels through more than 40 passages. Fig. 1A,B shows single Ca^{2+} channel activity of α_1-transfected CHW cells (α_1 cell or α_1 channel) and α_1/β-transfected CHW cells (α_1/β cell or α_1/β channel) respectively. They were measured in the cell-attached mode during repetitive voltage-clamp pulses from the holding potential of −80 mV to the 0 mV test potential, at a rate of 0.33 Hz. The inward deflections were short with an amplitude of about −1.0 pA (Fig. 1A) while the α_1/β channel occasionally exhibited activities of varying duration (Fig. 1B). In addition to the majority of frequent openings with a large amplitude (major openings), the α_1/β channel occasionally exhibited activities with smaller unitary amplitudes (minor openings, indicated by arrows). The number of minor openings with small amplitudes comprised 0.1–0.5% of the total number of openings. The average mean open time (at 0 mV) for the major openings was 0.33 ± 0.05 ms (6 patches) for the α_1 channel and 0.39 ± 0.04 ms (14 patches) for the α_1/β channel (data not illustrated). To study the sensitivity of the expressed channels to a DHP agonist and to more precisely measure amplitudes of single unitary currents, we recorded channel activity in the presence of Bay-K 8644 in the pipette (Fig. 1C,D). Here, the open channel duration was prolonged. Mean open times (at 0 mV) was 30.8 ± 14.8 ms (14 patches) in the α_1 channel and 37.8 ± 18.8 ms in the α_1/β channel (9 patches), which indicated that the expressed channels were indeed DHP-sensitive (L-type Ca^{2+}) channels. In the presence of Bay-K 8644, single channel currents were measured when the test potential was stepped from −10 to +30 mV and obtained I-V relationships are drawn in Fig. 1E,F. The slope conductance of the large openings (major openings) was 20.6 pS for the α_1 channel and 21.3 pS for the α_1/β channel. This result, together with other pooled data, indicated that the slope conductance of the α_1 channel was not affected by coexpression of the β subunit: the average conductance value was 22.5 ± 0.2 pS ($n = 12$) for the α_1 alone and 22.2 ± 0.2 pS ($n = 25$) for the α_1/β channel.

To determine whether the α_1 channel alone is able to produce channel activity with various unitary amplitudes and whether the coexpression of the β subunit is a prerequisite for the formation of conductance sublevels, we measured channel currents using ramp voltage-clamp methods in a cell-attached configuration, as illustrated in Fig. 2A. Recordings were made by introducing a ramp voltage command where the potential was promptly depolarized every 5 s from −80 mV to +40 mV and slowly repolarized at −0.1 V/s. Fig. 2A illustrates selected current sweeps of various amplitudes: sweeps a–d were obtained from an α_1 channel while sweeps e–h were from an α_1/β channel. The majority of channel activity exhibited current traces similar to those shown in

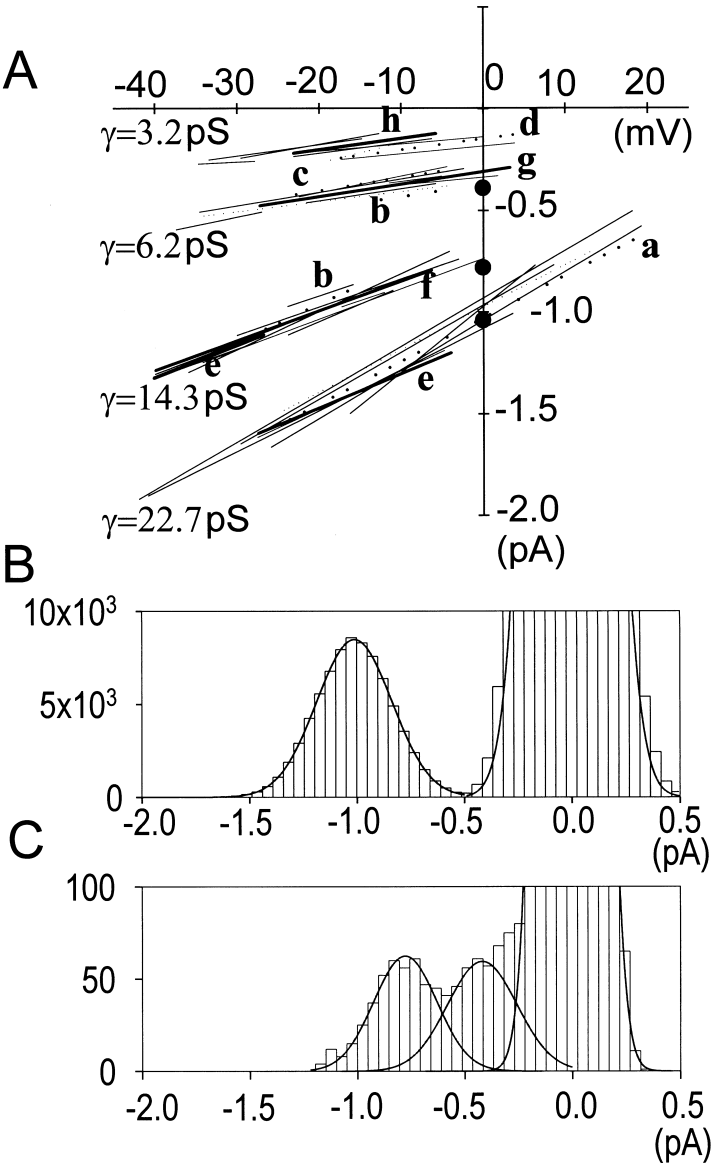

Fig. 3. Four single channel conductances of α_1 and α_1/β channels (A), and amplitude histograms obtained from an α_1 channel (B, C). A: Regression lines of the unitary current amplitudes plotted as a function of membrane potential were obtained from current traces such as those shown in Fig. 2. Extension of the regression line conformed to the duration of each burst opening. Solid lines were from α_1/β channels, and dotted lines from α_1 channels. Bold lines (a–h) correspond to those of the openings illustrated in Fig. 2. Regression lines were divided into four groups, with conductances (γ) of 22.7 pS, 14.3 pS, 6.2 pS and 3.2 pS. Three filled circles indicate unitary current amplitudes of three distinct channel activities at 0 mV calculated by the step protocol and the histograms in B and C. B: All points amplitude histogram of the channel activities at 0 mV constructed by a representative patch with a single α_1 channel. Unitary current amplitude of the majority of the openings (1.04 pA) was determined by Gaussian curve fit to the histogram constructed by 302 non-null sweeps out of 781 total sweeps. C: Histogram and Gaussian fits of the channel activities from six visually selected sweeps in the same patch in B with only smaller channel amplitude than 0.5 pA, determining the mean amplitudes of 0.78 pA and 0.39 pA.

sweeps a or e. Current types similar to traces b, c, d, f, g and h were uncommonly observed. All sweeps in Fig. 2A were superimposed using the magnified vertical scales in Fig. 2B,C. In addition to the majority of openings (O), three different sublevels of openings (S1, S2, S3) were identified. Because all channel activities recorded here consist of long lasting openings that had never been observed either in mock transfected CHW cells or in α_1 or α_1/β cells examined in the absence of Bay-K 8644, it was assumed that those large or small channel activities were derived from the DHP-sensitive component. We illustrate that the α_1 channel alone can produce four different open state levels, since current traces recorded from the α_1 cell (a, b, c and d in panel A) contained all four channel conductance levels (O, S1, S2 and S3) as demonstrated in panels B and C.

To more precisely determine the slope conductance of each open state, a linear regression line was made by using least squares fit to the ramp current amplitude. This line was plotted against membrane potentials in Fig. 3A, so that the straight line slope indicates single channel conductance of each channel current. Regression lines thus obtained were sorted into four groups according to their slopes irrespective of the presence or absence of β subunit coexpression indicating that the cardiac α_1 channel per se may produce at least

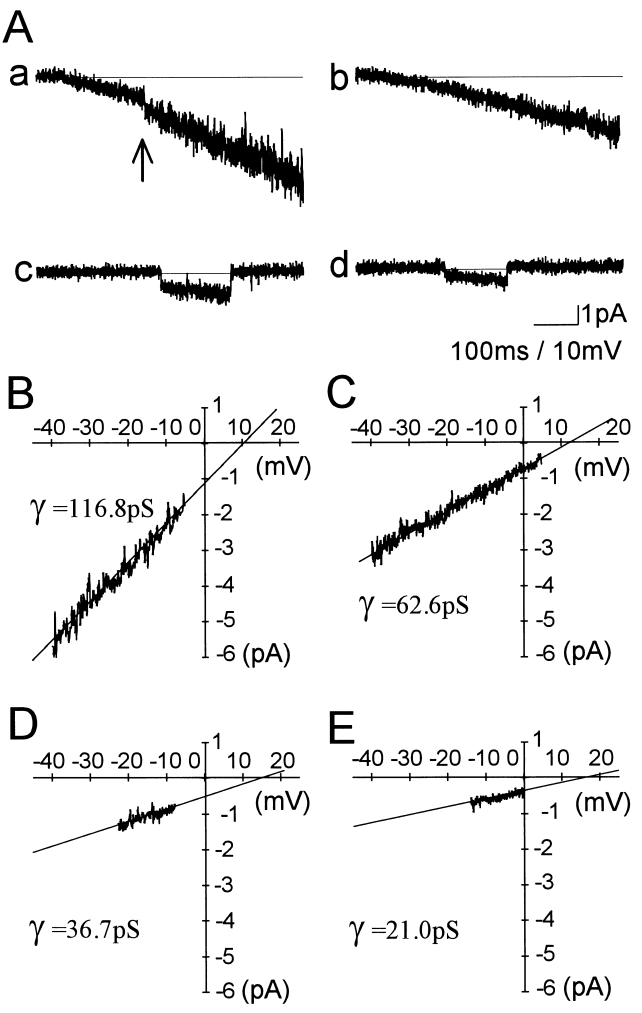

Fig. 4. Four conductance states of α_1 channel current recorded using 110 mM Na^+ as a charge carrier in the pipette also containing Bay-K 8644 (5 μM). The same ramp voltage clamp protocol from Fig. 2 was used. Here, EGTA (1 mM) was added to the pipette and BAPTA-AM (1 mM) was added to the bath solution (see Section 2) to chelate external and internal Ca^{2+}, respectively. In addition, the pipette solution pH was adjusted to 9.0 to avoid proton-Na^+ interaction through the channel. Actual current traces (Aa–d) and regression of each trace show maximal conductance level (Aa, B; 116.8 pS), and three smaller conductance levels of 62.6 pS (Ab, C), 36.7 pS (Ac, D) and 21.0 pS (Ad, E). In B, only a component of larger amplitude in Aa is shown and fitted. The majority of the channel activity showed amplitudes similar to those shown in Aa (larger amplitude) and B. For clarity, a smoothing algorithm was applied to the open channel activity (B–E). Note that a small channel amplitude transitionally increased to the largest one during the ramp in panel Aa (indicated by an arrow).

four different conducting states. The presence or absence of the β subunit did not affect the evolution or maintenance of subconductance states. To compare the ramp current amplitudes and the step-pulse current amplitudes, and to investigate the possible contribution of the subconductance openings to the whole channel activity, we constructed a histogram of all sampled points of the α_1 channel activity at 0 mV in Fig. 3B. Because more than 98% of non-null sweeps were occupied by large channel openings, any smaller channel events were not clearly resolved. Regression lines of the largest channel activity crossed over at −1.0 pA at the potential of 0 mV (Fig. 3A), while the determined mean unitary amplitude of the largest α_1 channel at 0 mV was 1.04 pA (Fig. 3B). Furthermore, the largest conductance (22.7 pS) in Fig. 3A was identical to that determined from Gaussian fits to the amplitude histograms for the various test potentials (22.5 pS for α_1 and or 22.2 pS for α_1/β, Fig. 1E,F). Three other subconductances were calculated by the regression of the ramp amplitudes to be 14.3 pS, 6.2 pS, and 3.2 pS (Fig. 3A). Extrapolation of all four regression lines led to a cross-over at +60 mV in the membrane potential. An amplitude histogram generated only by smaller channel events clearly showed two populations of the channel activities around 0.78 pA and 0.39 pA, and apart from these two populations, unfitted events were observed at bins between −0.35 pA and −0.25 pA (Fig. 3C).

Using the threshold detection algorithm, the number of channel openings in these four conductance levels in the absence of Bay-K 8644 were counted at 0 mV using step pulse protocol. In the α_1 channels, of a total of 22 110 sweeps in 34 patches, 15 014 sweeps showed no activity (null). The remaining 7096 sweeps showed 59 760 activities of the 23 pS current, 118 activities of the 14 pS current, 210 activities of the 6 pS current and 72 activities of the 3 pS current. In the α_1/β channels, of the total of 13 140 sweeps in 27 patches, 4983 sweeps showed null. The remaining 8157 sweeps showed 139 480 activities of the 23 pS current, 281 activities of the 14 pS current, 446 activities of the 6 pS current and 371 activities of the 3 pS current. We then counted data points for the 1.04 pA openings (or 22 pS), 0.78 pA openings (or 14 pS) and 0.39 pA openings (or 6 pS) at the potential of 0 mV, in the presence and absence of β subunit, by integration of each Gaussian fitting curve under the effect of 5 μM Bay-K 8644 (such as in Fig. 3B,C). When the line integral for the Gaussian fitting curve for 1.04 pA openings was assigned a value of 1.00, those for 0.78 pA openings and 0.39 pA openings were 7.35 ± 1.67 ($\times 10^{-3}$) and 6.04 ± 2.75 ($\times 10^{-3}$) for the α_1 channel ($n = 5$), and 8.84 ± 1.80 ($\times 10^{-3}$) and 5.78 ± 1.69 ($\times 10^{-3}$) for the α_1/β channel ($n = 6$), respectively. Taken together, the individual contributions of these three subconductances for the total Ca^{2+} activity at 0 mV were assumed to be less than 1% in terms of events number and charge movements in cases of the α_1 and α_1/β channel.

The mean open duration of a 14 pS subconductance opening measured at 0 mV was 0.35 ± 0.14 ms (118 events: α_1 channel) and 0.38 ± 0.11 ms (182 events: α_1/β channel). We did not measure the open time duration in openings smaller than the 14 pS conductance level, because kinetic analysis for smaller openings could involve considerable error due to poor signal-to-noise ratios.

We wondered whether the formation of four different conducting states depends on the specific carrier ion, in this case, Ba^{2+}. One way to answer this question would be to see whether the subconductance level(s) can be produced using different cations as a charge carrier. This was tested in experiments illustrated in Fig. 4. The same ramp voltage protocol was used as in Fig. 2, instead of 110 mM Ba^{2+} we used 110 mM Na^+ at the pH of 9.0 in the pipette. Under these conditions, the α_1 channel revealed four different conductances similar to those seen with Ba^{2+} as a charge carrier. With Na^+ as a charge carrier, the vast majority of sweeps (690 sweeps) had openings with 117.3 ± 2.8 pS conductance, and occasionally, conductances of 64.3 ± 3.4 pS (13 sweeps), 35.5 ± 2.0 pS (7 sweeps), and 21.5 ± 0.8 pS (5 sweeps) were observed out of

2065 sweeps in four patches in total. Moreover, transformation of one open state (smaller conductance) into another (full conductance) was again observed under the pipette solution of 110 mM Na^+. As expected, Na^+, a monovalent alkali ion, exerted high permeability through the α_1 Ca^{2+} channel. When the highest (117 pS) conductance was assigned a value of 100%, the other three conductances were calculated to be 55%, 30%, and 18%, respectively. These three ratios were in agreement with those calculated from three subconductances measured with Ba^{2+} as a charge carrier, i.e. 63%, 27%, and 14%, respectively.

4. Discussion

Using the cDNA of DHP-sensitive L-type Ca^{2+} channel α_1 subunit derived from rabbit cardiac muscle, the present study demonstrated that the channel expressed in the CHW cells exhibited four different levels of conductance (22.7, 14.3, 6.2 and 3.2 pS) when 110 mM Ba^{2+} was used as a charge carrier. Multiple levels could be seen in the absence of Bay-K 8644. However, these levels were easier to observe in the presence of the DHP agonist, which increased mean open times in all four conductance levels. This finding indicates that the α_1 channel was sensitive to the DHP agonist at every level of conductance. Considering that DHPs bind to the extracellular portion of the transmembrane helix of III S6 and IV S6 of the α_1 subunit [1], it is highly likely that DHP exerts its specific effect on all four conducting states via allosteric modulation. Because we have already confirmed that untransfected CHW cells did not express detectable mRNA for Ca^{2+} channel β subunit [17], it is unlikely that α_1-transfected cells were comprised of endogenous β subunit of the Ca^{2+} channel.

The existence of multiple conductances in the L-type Ca^{2+} channels has long been recognized in cardiac preparations. Chen and Hess reported a 17 pS sublevel in the guinea pig heart [20]. Conductance sublevels were also seen in Ca^{2+} channels of various tissues other than heart muscles. In excised patches from the vascular smooth muscle cells, L-type Ca^{2+} channels with 8 and 15 pS conductances have been reported [21]. There are also reports of sublevels having 50–70% of the major conductance in cell-attached patches of skeletal muscle cells [22]. In contrast to channels located in native membranes, multiple conductance levels are more likely to be observed in Ca^{2+} channels reconstituted into lipid bilayers [23–26].

Nevertheless, the mechanism(s) responsible for the appearance of different conductances in DHP-sensitive Ca^{2+} channels are not known. Although it is possible that the α_2/δ subunit somehow modulates conductance of the α_1 subunit, our study clearly demonstrates that the α_1 subunit per se is able to lead to the formation of, at least, four different conducting states. It has been shown that an increase in extracellular protons promotes the appearance of otherwise infrequent different conductance states [27]. However, we could not eliminate the development of four conductance levels by use of a low, external proton concentration of 10^{-9} M (pH of 9.0), in combination with 110 mM Na^+ as a charge carrier (Fig. 4).

The magnitude of the Ca^{2+} channel conductance has been used to sort out the differing types of Ca^{2+} channel in some cells [28]. The present study indicates that the presence of multiple sublevels in the same, single α_1 channel may present difficulty in the analysis of the Ca^{2+} channel. Problems of single channel analysis include the fact that different conductance states may exhibit differing life times, and that differing voltages may produce differing conductance levels. The former possibility seems to be excluded by our experiments, because the mean open times (in the absence of Bay-K 8644 in the pipette) were similar for the openings of the four conductance levels and between the α_1 and α_1/β channels. However, details of the kinetic changes remain to be determined, since the present study adequately resolved only the long lasting transitions. The second problem also require further elucidation, since the majority of current traces (except for the ramp-pulse protocol and the data in Fig. 1) were obtained at a fixed test potential of 0 mV.

Transformation of one state into another, for example, transitions from 23 pS openings to 14 pS openings, while extremely rare, have been observed with 110 mM Ba^{2+} as a charge carrier (Fig. 2Ab,e, indicated by arrows). Moreover, a transition from 63 pS opening to 117 pS opening was also observed with 110 mM Na^+ as a charge carrier (Fig. 4Aa, indicated by an arrow). This is the most convincing evidence that subconductances arose from the same, single Ca^{2+} channel. Additional support for this recognition is the observation that all regression lines converged at the same reversal potential of +60 mV. However, in the absence of the agonist (Bay-K 8644), we observed only a single case of the transition from 22 pS to 14 pS, and from 14 pS to 6 pS.

The functional role of the Ca^{2+} channel β subunit, coexpressed with the α_1 subunit, has been studied with regard to current amplitude, rate of activation, rate of inactivation, number of DHP binding sites, and even the 'maturation' of channels [6,7,11,12]. In terms of the formation of the sublevels, however, the role of the β subunit has not yet been studied. In the present study, coexpression of the β subunit did not affect single channel conductances nor did it change the population ratio among the three smaller subconductances. Inclusion of the β subunit decreased the number of null sweeps and increased the number of openings per sweep of the major conductance (23 pS). Because coexistence of the β subunit did not increase the number of openings in all three subconductance levels or proportional ratios for the line integrals for fitting curves of the two smaller conductances (14 and 6 pS) to that of 23 pS openings in the amplitude histograms, it is assumed that β subunit equally favors all three subconductances as is the case of the 23 pS full conductance regardless of the presence of a dihydropyridine agonist.

It is possible that the evolution of the different levels of conductance is influenced by the cell's metabolic state, because the activity of DHP-sensitive Ca^{2+} channels is known to be affected by phosphorylation [29–31]. However, since our present study did not include examination of the effect of activation or inhibition of cAMP-dependent protein kinase, we could not draw a conclusion regarding the contribution of phosphorylation to the appearance of subconductances. Both the cardiac α_1 and β subunits contain multiple potential phosphorylation sites [31], although it is still not known which subunit(s) of the DHP-sensitive Ca^{2+} channel have the greatest responsibility for regulating the channels mediated by protein phosphorylation. Further studies are required to understand how each subunit (and its phosphorylation) may modulate the evolution of subconductance(s) and the full conductance in the Ca^{2+} channels.

In conclusion, we demonstrated that the cardiac α_1 subunit of the DHP-sensitive Ca^{2+} channel exhibits four distinct states of conductance, and that these conductances are unaffected by the presence or absence of the cardiac β subunit. The underlying molecular mechanism remains to be studied.

Acknowledgements: This study was supported in part by the Japan Heart Foundation and IBM Japan Research Grant (to K.O.), and Grants-in-Aid for Scientific Research (07807008, 09670049) from the Ministry of Education, Science, Sports and Culture of Japan (to K.O.).

References

[1] Catterall, W.A. and Striessnig, G. (1992) Trends Pharmacol. Sci. 13, 256–262.
[2] Singer, D., Biel, M., Lotan, I., Flockerzi, V., Hofmann, F. and Dascal, N. (1991) Science 253, 1553–1557.
[3] Wei, X., Perez-Reyes, E., Lacerda, A.E., Schuster, G., Brown, A.M. and Birmbaumer, L. (1991) J. Biol. Chem. 266, 21943–21947.
[4] Zong, S., Zhou, J. and Tanabe, T. (1994) Biochem. Biophys. Res. Commun. 201, 1117–1123.
[5] Ruth, P., Röhrkasten, A., Biel, M., Bosse, E., Regulla, S., Meyer, H.E., Flockerzi, V. and Hofmann, F. (1989) Science 245, 1115–1118.
[6] Hullin, R., Singer-Lahat, D., Freichel, M., Biel, M., Dascal, N., Hofmann, F. and Flockerzi, V. (1992) EMBO J. 11, 885–890.
[7] Nishimua, S., Takeshima, H., Hofmann, F., Flockerzi, V. and Imoto, K. (1993) FEBS Lett. 324, 283–286.
[8] Perez-Garcia, M.T., Kamp, T.J. and Marban, E. (1995) J. Gen. Physiol. 105, 289–305.
[9] Varadi, G., Lory, P., Schultz, D., Varadi, M. and Schwartz, A. (1991) Nature 352, 159–162.
[10] Lory, P., Varadi, G., Slish, D.F., Varadi, M. and Schwart, A. (1993) FEBS Lett. 315, 167–172.
[11] Lacerda, A.E., Kim, H.S., Ruth, P., Perez-Reyes, E., Flockerzi, V., Hofmann, F., Birmbaumer, L. and Brown, A.M. (1991) J. Biol. Chem. 266, 21943–21947.
[12] Castellano, A., Wei, X., Birmbaumer, L. and Perez-Reyes, E. (1996) J. Biol. Chem. 268, 12359–12366.
[13] Lacinová, L., Ludwig, A., Bosse, E., Flockerzi, V. and Hofmann, F. (1995) FEBS Lett. 373, 103–107.
[14] McDonald, T.F., Pelzer, S., Trautwein, W. and Pelzer, D.J. (1994) Physiol. Rev. 74, 365–507.
[15] Ono, K., Gondo, N., Wada, T., Mannen, K. and Arita, M. (1996) Circulation 94, (Suppl.) 1–224.
[16] Yatani, A., Wakamori, M., Niidome, T., Yamamoto, S., Tanaka, I., Mori, Y., Katayama, K. and Green, S. (1995) Circ. Res. 76, 335–342.
[17] Masaki, H., Green, S.A., Heiny, J.A. and Yatani, A. (1995) Receptor 5, 219–231.
[18] Perez-Reyes, E., Castellano, A., Kim, H.S., Bertrand, P., Baggstrom, E., Lacerda, A.E., Wei, X. and Birmbaumer, L. (1992) J. Biol. Chem. 267, 1792–1797.
[19] Hamill, O.P., Marty, A., Neher, E., Sakmann, B. and Sigworth, F.J. (1981) Pflügers Arch. 391, 85–100.
[20] Chen, C. and Hess, P. (1987) J. Physiol. 390, 80.
[21] Ohya, Y. and Sperelakis, N. (1989) Pflügers Arch. 414, 257–264.
[22] Lansman, J.B. (1990) J. Gen. Physiol. 95, 679–696.
[23] Ma, J. and Coronado, R. (1988) Biophys. J. 53, 387–395.
[24] Talvenheimo, J.A., Worley III, J.F. and Nelson, M.T. (1987) Biophys. J. 52, 891–899.
[25] Yatani, A., Imoto, Y., Codina, J., Hamilton, S.L., Brown, A.M. and Birnbaumer, L. (1988) J. Biol. Chem. 263, 9887–9895.
[26] Mejía-Alvarez, R., Fill, M. and Stefani, E. (1991) J. Gen. Physiol. 97, 393–412.
[27] Prod'hom, B., Pietrobon, D. and Hess, P. (1989) J. Gen. Physiol. 94, 23–42.
[28] Nowycky, M., Fox, A.P. and Tsien, R.W. (1985) Nature 316, 440–443.
[29] Rane, S.G. and Dunlap, K. (1986) Proc. Natl. Acad. Sci. USA 83, 184–188.
[30] Trautwein, W., Cavalié, A., Flockerzi, V., Hofmann, F. and Pelzer, D. (1987) Circ. Res. 61, (Suppl. I) I17–I23.
[31] Hosey, M.M., Chien, A.J. and Puri, T.S. (1997) Trends Cardiovasc. Med. 29, 427–450.